Journal of Applied Sciences and Nanotechnology

Journal homepage: https://jasn.uotechnology.edu.iq/

An Alternative Method for Estimating the Phase Fraction of Multiphase Nanomaterials: Analysis from X-ray Diffraction

[1]Peverga R. Jubu*, [2]Khaled M. Chahrour, [3]Yushamdan Yusof, [4]A. Nathan-Abutu, [5]V. M. Igba, [6]E. Danladi, [3]O. S. Obaseki, [1]M. B. Ochang, [1]W. V. Zhiya, [3]F. K. Yam*

[1]Department of Physics, Joseph Sarwuan Tarka University Makurdi (University of Agriculture Makurdi) – Nigeria

[2]Department of Mechanical Engineering, Faculty of Engineering, Karabuk University – Turkey

[3]School of Physics, Universiti Sains Malaysia – Malaysia

[4]Materials Science Department, Centro de Investigaci´on en Materiales Avanzados – Mexico

[5]Facultad de Ciencias Quimicas, Universidad Autonoma de Coahuila – Mexico

[6]Department of Physics, Federal University of Health Sciences Otukpo – Nigeria

Article information

Article history:
Received: June, 24, 2023
Accepted: August, 06, 2023
Available online: September, 10, 2023

Keywords:
Phase fraction,
Nanocomposite,
Spurr-Myers relation

Corresponding Authors:
Peverga R. Jubu
peverga.jubu@uam.edu.ng

F. K. Yam
yamfk@usm.my

Abstract

The presence of multiple phases/ components within a nanocomposite material impacts the properties of a nanomaterial. Therefore, there is a need to estimate the phase fraction of each component present in a sample. Spurr-Myers proposed a valuable formula for estimating the rutile and anatase phase fraction of a TiO_2 sample from X-ray diffraction. However, this formula is dedicated to TiO_2 and is inapplicable to samples that contains more than two phases. The present research work proposed a simple method for quantifying the phase fraction of all types of nanomaterials that consist of two or more phases. Precision/ accuracy test carried out by multiplying the grand total intensity of all the diffraction peaks present in a sample with the value of the phase fraction of individual components showed that the proposed method gave precision values that were equivalent to the sum of the intensity of the peaks of each component. Whereas the S-M gave precision values that were significantly inconsistent with the sum of the intensity of the peaks of each component. The study showed that the proposed method was valid for a wide range of 2θ values and can be deployed to obtain reasonable and reliable values of phase fraction that could assist to understand the material phase fraction-properties relationship.

DOI: 10.53293/jasn.2023.7002.1222, Department of Applied Sciences, University of Technology

1. Introduction

A nanocomposite material is a mixture of different nanomaterials (materials with at least one of its dimensions falling in the nanometer scale range of (1-100 nm). In other words, a nanocomposite is a multiphase solid nanomaterial (in the form of nanoparticles or thin film) in which one of the components has one, two, or three

dimensions ≤ 100 nm. A nanocomposite retains the unique characteristics of each component. Nanocomposites offer excellent materials properties that may be difficult to achieve from the individual component [1] and lead to the enhancement of device performance due to the synergistic effect between the components/ phases [2-6]. One of the interesting characteristics of a nanocomposite is the formation of a heterojunction (which aids charge carrier separation and transport) at the interface between the phases [6-8]. Nanocomposites such as ZnO/Ga_2O_3, α-Fe_2O_3/CuO, Ga_2O_3/GaN, $MoO_3/TiO_2/Ti_3C_2T_x$, and Ga_2O_3/TiO_2 have been produced and applied for photoelectrochemical water splitting, photodetection, chemical sensing, and biological treatment against bacterial [6-10]. A nanocomposite material is a mixture of different nanomaterials (materials with at least one of its dimensions falling in the nanometer scale range of (1-100 nm). In other words, a nanocomposite is a multiphase solid nanomaterial (in the form of nanoparticles or thin film) in which one of the components has one, two, or three dimensions ≤ 100 nm. A nanocomposite retains the unique characteristics of each component. Nanocomposites offer excellent materials properties that may be difficult to achieve from the individual component [1] and lead to the enhancement of device performance due to the synergistic effect between the components/ phases [2-6]. One of the interesting characteristics of a nanocomposite is the formation of a heterojunction (which aids charge carrier separation and transport) at the interface between the phases [6-8]. Nanocomposites such as ZnO/Ga_2O_3, α-Fe_2O_3/CuO, Ga_2O_3/GaN, $MoO_3/TiO_2/Ti_3C_2T_x$, and Ga_2O_3/TiO_2 have been produced and applied for photoelectrochemical water splitting, photodetection, chemical sensing, and biological treatment against bacterial [6-10]. Because of their improved materials characteristics due to the heterojunction formation and synergetic effect between the phases, it is desirable to quantify how much a component is present in a synthesized sample. Many measurement techniques have been employed to calculate the phase fraction (PF) in solid nanomaterial, including electron backscatter diffraction [16, 17], energy dispersive synchrotron X-ray diffraction [18], neutron diffraction [19], and X-ray diffraction (XRD) analysis [2, 20-23]. The PF of the components present in a sample can be calculated from experimental data derived from the various measurement techniques. The Rietveld refinement was the first general method that was proposed for PF analysis. The method was published in 1967 [24]. The Rietveld method can be applied to all types of natural and synthetic materials. It can be performed on both multiphase crystalline and amorphous materials [25]. The Rietveld method is a full-profile fitting technique that considers the entire diffraction pattern of a sample for quantitative PF analysis [26, 27]. This makes the method more reliable than traditional methods that utilize a small, pre-selected set of integrated intensities. The wide acceptability of the Rietveld method for quantitative phase analysis is evident in the many publications on different classes of materials [26, 28–31]. Several researchers do not use the Rietveld method despite its high accuracy and widespread acceptability, probably because the idea is unclear. The authors who have applied this method do not clearly present the simplified step-by-step approach to how they used the Rietveld method to calculate the PF in a sample [25–27, 29]. Therefore, there is a need to develop simpler or easier-to-understand methods for PF analysis. The method proposed by Spurr and Myers (S-M) in the year 1957, about a decade before Rietveld's method, was the first quantitative approach for estimating the PF of the various components present in a sample. The method was proposed for estimating the PF of rutile and anatase from the XRD data of a TiO_2 nanomaterials [21]. The S-M formula (Eqs. 1, 2) has remained the commonest method for quantifying the PF of TiO_2 samples for decades.

$$\boldsymbol{f_A}(\%) = \frac{\mathbf{0.79}\boldsymbol{I_A}}{\boldsymbol{I_R} + \mathbf{0.79}\boldsymbol{I_A}} \times \mathbf{100} \quad \textbf{(1)}$$

$$\boldsymbol{f_R}(\%) = (\mathbf{1} - \boldsymbol{f_A}) \times \mathbf{100} \quad \textbf{(2)}$$

where f_A is the PF of anatase, f_R is the PF of rutile, I_A is the strongest intensity of anatase, and I_R is the strongest intensity of rutile. Unlike the Rietveld method, the S-M relation is an averaging method that considers only the strongest/ predominant diffraction peaks of the rutile and anatase phases present on the XRD pattern of a TiO_2 sample. Aside been dedicated to the TiO_2 material, the S-M relation is valid for a bi-phase TiO_2 sample, only, and cannot be deployed for a TiO_2 sample consisting of more than two phases.

Another widely used method for determining PF is that which considers the relative intensity ratio of the characteristic peaks of the phases present in a sample (Eqs. 3, 4) [32-35]. Just like the S-M method, the relative intensity ratio method considers only the predominant diffraction peak per component and does not use all the peaks present in a diffraction pattern. However, its advantage over the S-M method is that it can be applied to a sample that consists of two or more phases [32, 33]. The limitation of the two methods is that they consider only the intensities of the strongest diffraction peaks, thereby giving PF values that are not accurate. Overall, the Rietveld method is superior to the other two methods because it provides a more accurate result by fitting the entire diffraction pattern of a sample.

$$f_B = \frac{I_B}{I_B + I_C + I_D \pm \cdots} \times 100\% \quad (3)$$

$$f_C = \frac{I_C}{I_B + I_C + I_D \pm \cdots} \times 100\% \quad (4)$$

where f_B is the PF of phase B, f_C is the PF of phase C, I_B is the strongest intensity of component B, and I_C is the predominant intensity of component C. The PF of component D can be calculated in a similar manner, and so on [32-35]. An inference from the preceding paragraphs shows that there is a need to propose a simple but general method that can be used to estimate the PF of a multiphase nanomaterial. The proposed method, unlike the S-M and relative-intensity-ratio methods, should consider all the diffraction peaks to get an accurate estimate of the PF of the components in a sample. The proposed method should be applicable to all types of nanomaterials, like the Rietveld method. The present work proposes a typical method for estimating the PF of all kinds of nanocomposite materials that consists of two or more phases. The proposed method is general, unlike the S-M, which can only be applied to a bi-phase TiO_2 sample and cannot be used for other multiphase nanomaterials.

2. Experimental Procedure

2.1. Sample Preparation

Ga_2O_3/ZnO nanocomposite and TiO_2 films were used for this study. The TiO_2 film was synthesized by anodization and post-annealed at 450 ℃ as described in our previous report [20]. Prior to synthesis, a 0.127-mm thick Ti foil (purity 99.7%) was cut into a small piece of size 1 × 1 cm^2. The Ti foil substrate was washed by sonicating in methanol and acetone for 20 min, followed by bathing with deionized water, and subsequently dried in an oven. Anodization was carried out in a Teflon cubicle consisting of the Ti foil substrate as the anode and a platinum bar as the counter electrode connected to a Keithley model-2400 as the voltage source. An electrolyte prepared by mixing 0.1 wt% NH_4F, 2 wt% H_2O, and 98 wt% ethylene glycol was deployed for the reaction. A two-step anodization process was employed for the synthesis at room temperature under a direct current voltage for 2 h. The prepared TiO_2 layer was mechanically detached after the first-step anodization. The second-step anodization involved a repetition of the first-step synthesis. The fabricated film was immediately washed with deionized water and dried in the oven. The prepared film was annealed in a horizontal tube furnace at 550 ℃ under a supply of water vapour/ N_2 for 3 h. The water vapour was supplied as an oxygen source for the oxidation of the film. On the other hand, the N_2 gas was used as a carrier gas to supply the vapour into the reactor [20]. On the other hand, a two-step growth technique was used to prepare the Ga_2O_3/ZnO nanocomposite film. This was to ensure the solubility of ZnO and Ga_2O_3 in the gas phase to obtain a nanocomposite having prominent diffraction peaks of Ga_2O_3 and ZnO. Firstly, about 50 mg Ga_2O_3 powder (99.998% purity, Strem Chemical Inc.) was placed in a partially covered ceramic boat and loaded to the center/ hot zone of a horizontal tube chemical vapour deposition (CVD) system for decomposition at 950 ℃. The reactor was supplied with 100 sccm H_2 reducing gas to aid thermal decomposition for 60 min (where sccm is cubic centimeter per minute). The furnace was shut down and a coating could be seen on the inner walls of the boat. In the second step, 30 mg of ZnO powder (99.99% purity, Kock-Light Laboratories Ltd) was mechanically mixed with 10 mg Ga_2O_3 and placed in the Ga_2O_3-contaminated boat and transferred to the center zone of the CVD. Si(111) substrate of size 1 × 1 cm^2 was placed vertically on support and loaded downstream of the furnace at a separation of 24 cm from the precursor. The temperature of the furnace was raised from room temperature to 950 ℃, while flowing 100 and 600 sccm H_2 reducing gas and N_2 carrier gas, respectively, into the horizontal reactor. The deposition was sustained for a period of 60 min before the furnace was shut down. A coating could be seen on the substrate [36, 37].

2.2. Characterization

The prepared TiO_2 and Ga_2O_3/ZnO films were characterized using a PANalytical X'pert PRO MRD PW3040 high-resolution X-ray diffractometer (XRD) employing Cu-Kα (λ = 0.15406 nm) radiation. The XRD was operated at room temperature under a generator setting of 40 mA and 40 kV. The samples were scanned between the Bragg-Brentano geometry (θ-2θ) of 20–75° at the step size of 0.05° and scan time of 1.5 s. The divergence slit size of 0.2393°, receiving slit size of 0.1 mm, a focus-divergence distance of 91 mm, and a goniometer radius of 320 mm were deployed for optimum measurements [13]. Phase identification was carried out using a HighScore software attached to the XRD. The software was used to match the diffraction peaks with the database (Joint Committee on Powder Diffraction Standards (JCPDS)).

2.3. The proposed Method for PF Analysis of a Multiphase Nanomaterial

Unlike the S-M relation, the proposed method is a holistic approach that considers the intensities of all the prominent diffraction peaks on a measured sample. The proposed method for the PF analysis of multiphase nanomaterials makes the following assumptions: (i) The sum of the intensity of the diffraction peaks of a particular component/ phase is directly proportional to the weight/ density of this component contained on the measured sample [21, 38], according to Eq. 5. (ii) The sum of the intensity of all the diffraction peaks on a sample (irrespective of the component/ phase) is directly proportional to the overall weight of the nanomaterial contained in the sample (Eq. 6). (ii). The sum of the estimated PF of the various components found in a sample should be equal to 100, since PF can be expressed in percentage.

$$\boldsymbol{I_{sx} = K_1 w_x} \quad \textbf{(5)}$$

$$\boldsymbol{I_{gt} = K_2 w_o} \quad \textbf{(6)}$$

where I_{sx} is the sum of the intensity of all diffraction peaks belonging to a particular component x, w_x is the weight of component x contained in the sample, I_{gt} is the grand/ overall total of the intensity of all diffraction peaks contained in the sample, w_o is the overall weight of the nanomaterial on the sample being measured, and $K_1 = K_2$ is a constant equal to unity for the materials contained on the same measured sample [21, 38]. Dividing Eq. 5 by Eq. 6 yields,

$$\frac{\boldsymbol{K_1}}{\boldsymbol{K_2}} \cdot \frac{\boldsymbol{w_x}}{\boldsymbol{w_o}} = \frac{\boldsymbol{I_{sx}}}{\boldsymbol{I_{gt}}}$$

$$\therefore \boldsymbol{f_x = \frac{I_{sx}}{I_{gt}}} \quad \textbf{(7)}$$

where $\frac{w_x}{w_o} = f_x$ is the phase/ weight fraction of a particular component x.

Expressing Eq. (7) in percentage leads to Eq. (8)

$$\boldsymbol{f_x(\%) = \frac{I_{sx}}{I_{gt}} \times 100} \quad \textbf{(8)}$$

Eq. 8 can be employed to estimate the PF of all nanomaterials. Although S-M has derived a dedicated relationship for the PF analysis of TiO_2, Eq. 6 can alternatively be applied for the TiO_2 to provide an estimate of the PFs of rutile and anatase contained in a TiO_2 sample. It should be noted that the proposed method can be used for a nanocomposite having more than two phases, unlike the S-M method.

3. Results and Discussion

Fig. 1 shows XRD patterns of the synthesized TiO_2 film and Ga_2O_3/ZnO nanocomposite. The XRD pattern of TiO_2 (Fig. 1(a)) exhibits diffraction peaks belonging to anatase with the prefix A, and rutile with the prefix R, according to the Joint Committee on Powder Diffraction Standards (JCPDS) card nos. 01-071-1167 and 01-077-0442, respectively. The anatase TiO_2 peaks were more intense, indicating its dominance in the sample. The metallic titanium (Ti) peaks marked with the prefix T (according to JCPDS card no. 01-089-2782) were reflections from

the Ti foil substrate used for the TiO_2 synthesis. The strongest/ predominant crystallographic peaks for anatase and rutile were the A(101) and the R(004) planes, respectively. Meanwhile, the dominance of the anatase over rutile at the post-annealing temperature of 450 ℃ was consistent with the literature [11, 20, 39]. Fig. A1(a) reveals the surface micrograph of the anodized TiO_2 film, as contained in the Supporting Document. Meanwhile, Table S1 presents the elemental composition of the samples.

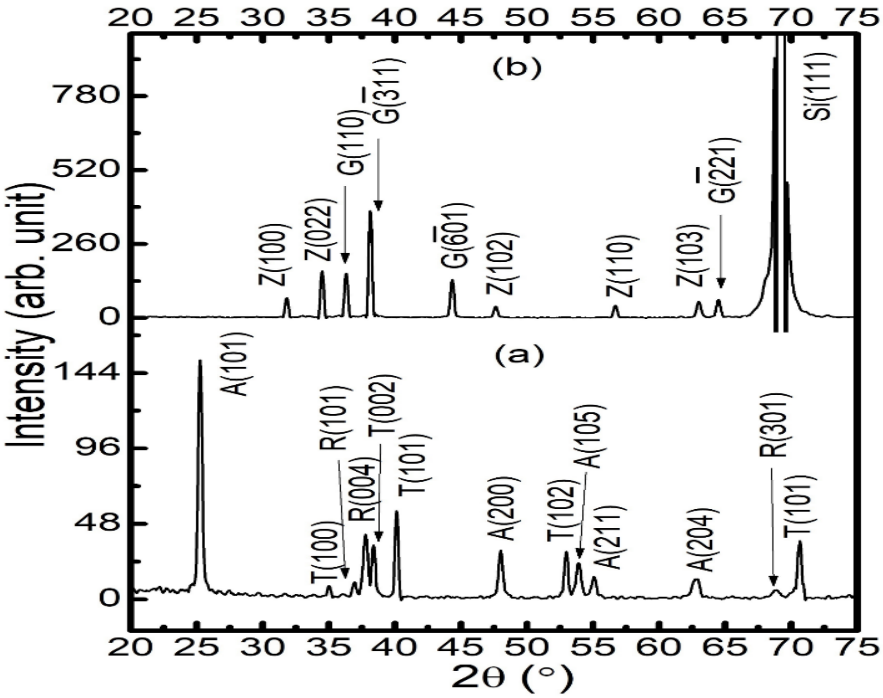

Figure 1: XRD patterns of the (a) anodized TiO_2 film; (b) CVD-grown Ga_2O_3/ZnO nanocomposite.

The XRD pattern for the nanocomposite (Fig. 1(b)) evinced crystallographic reflections belonging to the monoclinic phase of Ga_2O_3 (β-Ga_2O_3), which is marked with the prefix G and hexagonal ZnO marked with the prefix Z, according to JCPDS card nos. 00-043-1012 and 01-074-0534, respectively. ZnO peak intensities were relatively low compared to the β-Ga_2O_3 peaks due to the smaller amount of the ZnO material found in the sample [7] (Table S1). Fig. A1(b) shows the surface morphology of the CVD-grown Ga_2O_3/ZnO film. Peak profile analyses were carried out using the S-M relation and the proposed method for determining PF, and the results are presented in Table 1. According to the S-M method, the intensity I_A of the strongest anatase peak (A(101)) and the intensity I_R of the strongest rutile peak (R(004)) were used to calculate the PF of anatase (f_A) and rutile (f_R), respectively (Fig. 1, pattern (a)). The values of I_A and I_R were substituted into the S-M formula (Eq. (1)), and the resulting value of f_A was substituted into Eq. (2) to find f_R for the b-phase TiO_2 film. The proposed method (Eq. 8) was applied for the PF analysis of the bi-phase TiO_2 sample to check if it could provide values that were equivalent to those obtained from the TiO_2-dedicated S-M method (Table 1).

Table 1: Peak profile analysis of the various components on the TiO_2 and Ga_2O_3/ZnO films.

Sample	Material phase	I_{sx}	I_{gt}	PF (%) by the S-M method	PF (%) by the PM	Precision check = $I_{gt} \times$ PF	
						S-M	PM
TiO_2	Anatase	235.67	288.71	74.40	81.63	214.80	235.59
	Rutile	53.04		25.60	18.37	73.91	53.12
GO/ZO	β-Ga_2O_3	734.06	1112.51	63.93	65.98	711.23	734.03
	ZnO	378.45		36.07	34.02	401.28	378.48

Notes: - GO/ZO: Ga_2O_3 /ZnO, PM: proposed method.

It was evident that the sum of the intensities of anatase and rutile peaks were 235.67 and 53.04, respectively, which gives a grant total intensity of 288.71 for the TiO_2 sample. Meanwhile, the PF of anatase and rutile were calculated from the S-M method and found to be 74.4 and 25.6%, respectively. On the other hand, the proposed method gave PF values of 81.6 and 18.4% for anatase and rutile, respectively. This indicates a significant difference in the magnitude of the values of the PFs estimated from the two methods, which suggests that the proposed method may not be suitable for the TiO_2 material. Nevertheless, the precision/ success check showed that the proposed method could be suitable for the PF analysis of TiO_2 because it yielded (I_{gt} × PF) values that were equivalent to the sum of the intensity of the diffraction peaks for a particular component I_{sx} measured directly from the XRD pattern. Meanwhile, the (I_{gt} × PF) values obtained from the S-M method varied significantly from the observed I_{sx} for anatase and rutile that were measured directly from the XRD pattern. This suggests that the S-M is not infallible/ perfect, indicating that the proposed method can be an alternative for PF analysis. It should be noted that the sum of the XRD intensities from a particular component, *x*, is proportional to the amount of this material found in the measured sample. In other words, the component/ phase with a small or large amount on a sample will produce weak or strong diffraction peaks, respectively, from the XRD measurement [40-43]. The component with the highest amount or PF on a sample would produce the strongest diffraction peaks. Peak profile analysis of the Ga_2O_3/ZnO film using the proposed method gave PF value of 65.98 and 34.02% for the Ga_2O_3 and ZnO components, respectively. Precision check gave (I_{gt} × PF) values that were equivalent to the sum of the intensity of the diffraction peaks for a component I_{sx} measured directly from the XRD pattern. This also validates the proposed method for PF analysis. To confirm if the estimated values for the PF of the Ga_2O_3 and ZnO components were reasonable, the S-M was applied to the Ga_2O_3/ZnO film. Estimates show that the PF of Ga_2O_3 and ZnO was 63.93 and 36.07%, respectively. A comparison shows that the values of the PF for Ga_2O_3 and ZnO derived from the two methods vary slightly by a magnitude of 2.05. This suggest that the proposed method is reasonable. More interestingly, it can be applied to samples that consist of more than two phases. It is necessary to state that the scale of the 2θ axis must be kept between a wide range (to read all diffraction peaks) for the proposed method to yield a reasonable/ proper PF value. This is because the present method considers (sums up) all the prominent peaks contained in a sample, unlike the S-M relation that considers only the intensity of the strongest peak per component.

4. Conclusions

In summary, the present paper proposed a method for estimating the PF of a multiphase nanomaterial from XRD data. The Spurr-Myers method was employed to check the appropriateness of this proposed method for PF analysis. XRD data of anodized TiO_2 film and chemical vapour deposited Ga_2O_3/ZnO nanocomposite were used for this study. The proposed method was valid for a wide range of 2theta values and yielded reasonable PF values compared to those obtained from the Spurr-Myers method. Interestingly, the precision check showed that the estimated PF values obtained from the proposed method were more reasonable when compared to the values obtained from the Spurr-Myers method. Unlike the Spurr-Myers method that is dedicated to TiO_2 and is limited to a bi-phase sample, the proposed method can be applied to all nanomaterials consisting of two or more phases to give a reasonable idea about the PF of all components present on a sample.

Acknowledgement

The authors appreciate the Ministry of Higher Education Malaysia for the Fundamental Research Grant Scheme with Reference Code: (FRGS/1/2020/STG05/USM/02/4), and the Universiti Sains Malaysia (USM) for the financial and technical support for this research work.

Conflict of Interest

The authors declare that they have no conflict of interest.

References

[1] E. O. Miklicanin, A. Badnjevic, A Kazlagic, and M. Hajlovac, "Nanocomposites: A brief review," Health and Technology, vol. 10, no. 1, pp. 51-59, 2020. Doi: 10.1007/s12553-019-00380-x

[2] R. Su, R. Bechstein, L. Sø, R.T. Vang, M. Sillassen, B. Esbj€ornsson, A. Palmqvist, and F. Besenbacher, "How the anatase-to-rutile ratio influences the photoreactivity of TiO_2," J. Phys. Chem. C, vol. 115, pp. 24287–24292, 2011. Doi: 10.1021/jp2086768.

[3] X. Lv, J. Wua, J. Zhua, D. Xiaoa, and X. Zhangb, "A New method to improve the electrical properties of KNN-based ceramics: tailoring phase fraction," Journal of the European Ceramic Society, vol. 38, no. 1, pp. 85-94, 2017. Doi: 10.1016/j.jeurceramsoc.2017.08.016

[4] M.J. Mahmoodi, M.K. Hassanzadeh-Aghdam, and R. Ansari, "Overall thermal conductivity of unidirectional hybrid polymer nanocomposites containing SiO_2 nanoparticles," Int J Mech Mater Des, vol. 15, 539-554, 2019. Doi: 10.1007/s10999-018-9428-3

[5] I. Mccue, S. Xiang, K. Xie, and M.J. Demkowicz, "The effect of microstructure morphology on indentation response of Ta/Ti nanocomposite thin films," Metallurgical and Materials Transactions A, vol. 51A, pp. 5690-5677, 2020. Doi: 10.1007/s11661-020-05969-w

[6] U. Varshney, A. Sharma, P. Vashishtha, L. Goswami, and G. Gupta, Ga_2O_3/GaN Heterointerface-based self-driven broad-band ultraviolet photodetectors with high responsivity," ACS Appl. Electron. Mater. Vol. 4, no. 11, pp. 1-9, 2022. Doi: 10.1021/acsaelm.2c01362

[7] P.R. Jubu, F.K. Yam, and P.I. Kyesmen, "Structural, optical and electrochemical transient photoresponse properties of ZnO/Ga_2O_3 nanocomposites prepared by two-step CVD method," International Journal of Hydrogen Energy, vol. 46, pp. 33087-33097, 2021. Doi; 10.1016/j.ijhydene.2021.07.165

[8] P.I. Kyesmen, N. Nombona, and M. Diale, "Heterojunction of nanostructured α-Fe_2O_3/CuO for enhancement of photoelectrochemical water splitting," Journal of Alloys and Compounds, vol. 863, pp. 1-10, 2021. Doi: 10.1016/j.jallcom.2021.158724

[9] Y. Yao, Y. Han, M. Zhou, L. Xie, X. Zhao, Z. Wang, N. Barsan, and Z. Zhu, "MoO_3/TiO_2/$Ti_3C_2T_x$ nanocomposite-based gas sensors for highly sensitive and selective isopropanol detection at room temperature," **J. Mater. Chem. *A*, vol.** 10, pp. 8283-8292, 2022. Doi: 10.1039/D1TA11018G

[10] A.M. Ramesh, A. Gangadhar, M. Chikkamadaiah, and S. Shivann, "Hydrothermal synthesis of Ga_2O_3/TiO_2 nanocomposites with highly enhanced solar photocatalysis and their biological interest," Journal of Photochemistry and Photobiology, vol. 6, pp. 1-10, 2021. Doi: 10.1016/j.jpap.2021.100020

[11] K.M. Chahrour, P.C. Ooi, A.M. Eid, A.A. Nazeer, M. Madkour, C.F. Dee, M.F. Mohd Razip Wee, and A.A. Hamzah, "Synergistic effect of bi-phased and self-doped Ti^{+3} on anodic TiO^2 nanotubes photoelectrode for photoelectrochemical sensing," Journal of Alloys and Compounds, vol. 900, pp. 1-12, 2022. Doi: 10.1016/j.jallcom.2021.163496

[12] P.R. Jubu, F.K. Yam, O.S. Obaseki, and Y. Yusof, "Synthesis and characterization of gallium oxide in strong reducing growth ambient by chemical vapor deposition," Materials Science in Semiconductor Processing, vol. 121, pp. 1-6, 2021. Doi: 10.1016/j.mssp.2020.105361

[13] P.R. Jubu, F.K. Yama, and K.T. Low, "Feasibility study on synthesis of gallium oxide nanostructures on glass substrate by chemical vapor deposition," Thin Solid Films, vol. 710, pp.1-7, 2020. Doi: 10.1016/j.tsf.2020.138257

[14] M. Shaban, K. Abdelkarem, and A.M. El Sayed, "Structural, optical and gas sensing properties of Cu_2O/CuO mixed phase: effect of the number of coated layers and (Cr + S) co-doping," Phase Transitions, vol. 92, no. 4, pp. 1-8, 2019. Doi: 10.1080/01411594.2019.1581886

[15] M.-G. Ju, X. Wang, W.Z. Liang, Y. Zhao, and C. Li**, "**Tuning energy bandgap of gallium oxide crystalline to enhance photoelectrochemical water splitting: mixed-phase junctions," *J. Mater. Chem. A*, vol. 2, pp. 17005-17014, 2014. Doi: 10.1039/C4TA03193H

[16] A.W. Wilson, J.D. Madison, and G. Spanos, "Determination phase volume fraction in steels by electron backscattering diffraction," Scripta Materialia, vol. 45, pp. 1335-1340, 2001.

[17] W. Yin, X.J. Hao, A.J. Peyton, M. Strangwood, and C.L. Davis, "Measurement of permeability and ferrite/austenite phase fraction using a multi-frequency electromagnetic sensor," NDT and E International, vol. 42, no. 1, 64-68, 2009. Doi: 10.1016/j.ndteint.2008.01.009

[18] E. Polatidis, P. Frankel, J. Wei, M. Klaus, R.J. Comstock, A. Ambard, S. Lyon, R.A. Cottis, and M. Preuss, "Residual stresses and tetragonal phase fraction characterisation of corrosion tested Zircaloy-4 using energy

dispersive synchrotron X-ray diffraction," Journal of Nuclear Materials, vol. 432, pp. 102–112, 2013. Doi: 10.1016/j.jnucmat.2012.07.025

[19] R. Vaidyanathan, M.A.M. Bourke, and D.C. Dunand, "Phase fraction, texture and strain evolution in superelastic NiTi and NiTi–TiC composites investigated by neutron diffraction," Acta mater., vol. 47, no. 12, pp. 3353–3366, 1999.

[20] K.M. Chahrour, F.K. Yam, and A.M. Eid, "Water-splitting properties of bi-phased TiO_2 nanotube arrays subjected to high-temperature annealing," Ceramics International, vol. 46, no. 13, pp. 1-11. 2020. Doi: 10.1016/j.ceramint.2020.05.246

[21] R.A. Spurr, and H. Myers, "Quantitative analysis of anatase-rutile mixtures with an x-ray diffractometer," Chem., vol. 29, pp. 760–762, 1957. Doi: 10.1021/ac601259006

[22] B.M. Rao, and S.C. Roy, "Anatase TiO_2 nanotube arrays with high temperature stability," RSC Adv., vol. 4, pp. 1-8, 2014. Doi: 10.1039/c4ra05882h

[23] E. Amdeha, R.A. El-Salamony, and A.M. Al-Sabagh, "Enhancing the photocatalytic activity of Ga_2O_3–TiO_2 nanocomposites using sonication amplitudes for the degradation of Rhodamine B dye," Appl Organometal Chem., vol. 34, no. 2, pp. 1-11, 2019. Doi: 10.1002/aoc.5336

[24] H.M. Rietveld, "Line profiles of neutron powder-diffraction peaks for structure refinement," Acta Crystallographica, vol. 22, no. 1, 151–152, 1967. Doi: 10.1107/s0365110x67000234

[25] A.F.G.1. Giacomo, D. Gatta, R. Arletti, G. Artioli, P. Ballirano, G. Cruciani, A. Guagliardi, D. Malferrari, N. Masciocchi and P. Scardi**,** "Quantitative phase analysis using the Rietveld method: towards a procedure for checking the reliability and quality of the results," Periodico di Mineralogia, vol. 88, 147-151, 2019. Doi: 10.2451/2019PM870

[26] J.E.F.M. Ibrahim, M. Tihtih, E. Şahin, M.A. Basyooni, I. Kocserha, "Sustainable zeolitic tuff incorporating tea waste fired ceramic bricks: Development and investigation," *Case Studies in Construction Materials*, vol. 19, 1-6, 2023. Doi: 10.1016/j.cscm.2023.e02238

[27] P. Lemoine, C. Bourgès, T. Barbier, V. Nassif, S. Cordier and E. Guilmeau, "High temperature neutron powder diffraction study of the $Cu_{12}Sb_4S_{13}$ and $Cu_4Sn_7S_{16}$ phases," Journal of Solid State Chemistry, vol. 247, 83–89, 2017. Doi: 10.1016/j.jssc.2017.01.003

[28] A. Aatiq, R. Tigha, A. Attaoui, N. Nadi and A. El Bouar, "A Reitveld quantitative XRD phase-analysis of selected composition of the $Sr_{(0.5+x)}Sb_{(1-x)}Fe_{(1+x)}(PO_4)_3 (0 < x < 0.50)$ system," MATEC Web of Conferences, vol. 5, 1-3, 2013. Doi: 10.1051/matecconf/20130504018

[29] M. Hassan, M. Muazzam and T. Zelai, "Computational analysis of structural, electronic, magnetic and optical properties of $MgTM_2O_4$ (TM = Fe, V) Spinels," J. Electron. Mater. vol. 51, 4446–4455, 2022. Doi: 10.1007/s11664-022-09690-9

[30] K. Sabiruddin, J. Joardar and P.P Bandyopadhyay, "Analysis of phase transformation in plasma sprayed alumina coatings using Rietveld refinement," Surface and Coatings Technology, vol. 204, no. 20, 3248–3253, 2010. Doi: 10.1016/j.surfcoat.2010.03.026

[31] M. Baricco, S. Enzo, T.A. Baser, M. Satta, G. Vaughan and A.R. Yavari, "Amorphous/nanocrystalline composites analysed by the Rietveld method," Journal of Alloys and Compounds, vol. 495, no. 2, 377–381, 2010. Doi: 10.1016/j.jallcom.2009.11.024

[32] Y. Wang, L. Cai, Y. Li, Y. Tang and C. Xie, "Structural and photoelectrocatalytic characteristic of $ZnO/ZnWO_4/WO_3$ nanocomposites with double heterojunctions," Physica E: Low-Dimensional Systems and Nanostructures, vol. 43, no. 1, 503-509, 2010. Doi: 10.1016/j.physe.2010.09.005

[33] A.O. Juma, E.A.A. Arbab, C.M. Muiva, L.M. Lepodise, and G.T. Mola, 'Synthesis and characterization of CuO-NiO-ZnO mixed metal oxide nanocomposite," Journal of Alloys and Compounds, vol. 723, 866–872, 2017. Doi: 10.1016/j.jallcom.2017.06.288

[34] M. Bandi, V. Zade, S. Roy, A.N. Nair, S. Seacat, S. Sreenivasan and C.V. Ramana, "Effect of Ti induced chemical inhomogeneity on crystal structure, electronic structure and optical properties of wide bandgap Ga_2O_3," Crystal Growth & Design, vol. 30, 1-9, 2020. Doi: 10.1021/acs.cgd.9b00747

[35] D. Singh, B. Mallesham, A. Deshinge, K. Joshi, R. Ramadurai, and V. Balakrishnan, "Nanomechanical behavior of $Pb(Fe_{0.5-x}Sc_xNb_{0.5})O_3$ multiferroic ceramics*,"* Materials Research Express, vol. 5, no. 15, pp. 1-8, 2018. Doi: 10.1088/2053-1591/aade3b

[36] P.R. Jubu, O.S. Obaseki, F.K. Yam, S.M. Stephen, A.A. Avaa, A.A. McAsule, Y. Yusof, and D.A. Otor, "Influence of the secondary absorption and the vertical axis scale of the Tauc's plot on optical bandgap energy," Journal of Optics, vol. 9, pp. 1-10, 2022. Doi: 10.1007/s12596-022-00961-6

[37] P.R. Jubu, O.S. Obaseki, A. Nathan-Abutu, F.K. Yam, Y. Yusof, and M.B. Ochang, "Dispensability of the conventional Tauc's plot for accurate bandgap determination from UV–vis optical diffuse reflectance data," Results in Optics, vol. 9, pp. 1-7, 2022. Doi: 10.1016/j.rio.2022.100273

[38] S. Popovic, "Quantitative phase analysis by X-ray diffraction—doping methods and applications," Crystals, vol. 10, no. 27, pp. 1-15, 2020. Doi: 10.3390/cryst10010027

[39] N.R. Mathews, E.R. Morales, M. Cortés-Jacome, and J.T, "Antonio, TiO_2 thin films–Influence of annealing temperature on structural, optical and photocatalytic properties," *SoEn,* vol. 83, no. 9, 1499–1508, 2009. Doi: 10.1016/j.solener.2009.04.008

[40] P.R. Jubu, E.K. Yam, and L.H. San, "The influence of deposition temperature on the structural, morphological and optical properties of micro-size structures of beta-Ga_2O_3" Results in Physics, vol. 14, pp. 1-8, 2019. Doi: 10.1016/j.rinp.2019.102475

[41] F.A. Asim, Entessar, and H.A. Al-Mosawe, "Wafaa A. Hussain, The Medical Study of Denture Base Resin Poly(Methyl Methacrylate) Reinforced by ZnO and TCP Nanoparticles," Journal of Applied Sciences and Nanotechnology, vol. 2, no. 4, pp. 70-79, 2022. Doi. 10.53293/jasn.2022.4073.1137

[42] I. Benammar, R. Salhi, J. -L. Deschanvres, and R. Maalej, "Study of the Physico-Chemical Properties of Sol-Gel (Er, Yb) Doped TiO2 Nanoparticles Prepared with a Novel Protocol," Journal of Applied Sciences and Nanotechnology, vol. 3, no. 2, pp. 1-17, 2023. Doi: 10.53293/jasn.2023.6799.1208

[43] H.N. Abid, A. Al-Keisy, D.S. Ahmed, and S. Singh, "Preparation and Characterization of Bi2MO6 (M = Mo, W) for Antibacterial Activity," Journal of Applied Sciences and Nanotechnology, vol. 3, no. 2, pp. 32-40, 2023. Doi: 10.53293/jasn.2022.5250.1179